ornl

ORNL/TM-10983

OAK RIDGE
NATIONAL
LABORATORY

MARTIN MARIETTA

Gain and Electric Field Radiation Pattern Approximations for the E-Plane Horn Antenna

Paul D. Ewing

OAK RIDGE NATIONAL LABORATORY
CENTRAL RESEARCH LIBRARY
CIRCULATION SECTION
4500N ROOM 175
LIBRARY LOAN COPY
DO NOT TRANSFER TO ANOTHER PERSON
If you wish someone else to see this report, send in name with report and the library will arrange a loan.

OPERATED BY
MARTIN MARIETTA ENERGY SYSTEMS, INC.
FOR THE UNITED STATES
DEPARTMENT OF ENERGY

Printed in the United States of America. Available from
National Technical Information Service
U.S. Department of Commerce
5285 Port Royal Road, Springfield, Virginia 22161
NTIS price codes –Printed Copy: A04; Microfiche A01

This report was prepared as an account of work sponsored by an agency of the United States Government. Neither the United States Government nor any agency thereof, nor any of their employees, makes any warranty, express or implied, or assumes any legal liability or responsibility for the accuracy, completeness, or usefulness of any information, apparatus, product, or process disclosed, or represents that its use would not infringe privately owned rights. Reference herein to any specific commercial product, process, or service by trade name, trademark, manufacturer, or otherwise, does not necessarily constitute or imply its endorsement, recommendation, or favoring by the United States Government or any agency thereof. The views and opinions of authors expressed herein do not necessarily state or reflect those of the United States Government or any agency thereof.

ORNL/TM-10983
Distribution Category 406
Engineering, Equipment, and Instruments

Instrumentation and Controls Division

GAIN AND ELECTRIC FIELD RADIATION PATTERN APPROXIMATIONS FOR THE E-PLANE HORN ANTENNA*

Paul D. Ewing

Date Published: December 1988

*Thesis presented for the Master of Science Degree,
The University of Tennessee, Knoxville, 1987

Prepared by the
OAK RIDGE NATIONAL LABORATORY
Oak Ridge, Tennessee 37831
operated by
MARTIN MARIETTA ENERGY SYSTEMS, INC.
for the
U.S. DEPARTMENT OF ENERGY
Under Contract No. DE-AC05-84OR21400

MARTIN MARIETTA ENERGY SYSTEMS LIBRARIES
3 4456 0283921 2

ABSTRACT

A gain and electric (E) field radiation pattern approximation can be used to avoid the complex mathematics and computation methods typically required to calculate the gain and E field radiation pattern of the E-plane horn antenna. Using conventional techniques, the calculation of these antenna parameters involves solving the Fresnel integrals and the use of numerical integration. With the approximation model developed by the author, an estimate of the gain and E-plane radiation pattern can be determined using simple trigonometric terms.

The criterion used to evaluate the accuracy of the approximations was that the approximated values fall within 3 dB of the calculated values. Under this criterion, the results showed that the gain approximation holds for a flare angle of less than 10° for typical antenna dimensions and the E field radiation pattern approximation holds until the antenna's phase error approaches 60°.

TABLE OF CONTENTS

CHAPTER	PAGE
ABSTRACT	iii
LIST OF FIGURES	vii
LIST OF TABLES	ix
LIST OF SYMBOLS AND ABBREVIATIONS	xi
1. INTRODUCTION	1
1.1 Objective	1
1.2 Background	1
1.3 Description of E-Plane Horn Antenna	1
2. GAIN AND RADIATION PATTERNS	3
2.1 Aperture Distribution	3
2.2 Gain	3
2.3 Radiation Patterns	5
3. GAIN APPROXIMATION	8
3.1 Actual Gain	8
3.2 Approach to Gain Approximation	8
3.3 Magnitude of E Field from Isotropic Antenna	8
3.4 Linear Approximation of Wave Front from E-Plane Horn Antenna	9
3.5 Magnitude of E Field from E-Plane Horn Antenna	10
3.6 Gain Approximation Using E Field Magnitudes	12
3.7 Comparison of Actual Gain and Approximated Gain	12
4. RADIATION PATTERN APPROXIMATION	20
4.1 Actual Radiation Pattern	20
4.2 Approach to Radiation Pattern Approximation	20
4.3 Approximation of E-Plane Radiation Pattern	20
4.4 Comparison of Actual and Approximated Radiation Pattern	22
5. SUMMARY	32
6. REFERENCES	34

LIST OF FIGURES

FIGURE PAGE

1.1. The E-plane horn antenna 2

1.2. E and H fields in the E-plane horn antenna 2

2.1. Geometry of E-plane horn antenna 4

2.2. Relative E field radiation pattern 7

2.3. Relative H field radiation pattern 7

3.1. Geometry of linear approximation 10

3.2. Actual gain vs approximated gain--$a/\lambda = 0.5$, $b/\lambda = 2$, $\alpha = 1$ to $20°$ 17

3.3. Actual gain vs approximated gain--$a/\lambda = 0.5$, $b/\lambda = 3$, $\alpha = 1$ to $20°$ 17

3.4. Actual gain vs approximated gain--$a/\lambda = 0.5$, $\alpha = 2°$, $b/\lambda = 0.5$ to 6.0 18

3.5. Actual gain vs approximated gain--$a/\lambda = 0.5$, $\alpha = 5°$, $b/\lambda = 0.5$ to 6.0 18

3.6. Actual gain vs approximated gain--$a/\lambda = 0.5$, $\alpha = 10°$, $b/\lambda = 0.5$ to 6.0 19

3.7. Actual gain vs approximated gain--$a/\lambda = 0.5$, $\alpha = 15°$, $b/\lambda = 0.5$ to 6.0 19

4.1. E-plane horn antenna pattern 21

4.2. Geometry of E-plane radiation pattern approximation 21

4.3. Actual vs approximated radiated pattern--maximum phase error = 0° 29

4.4. Actual vs approximated radiated pattern--maximum phase error = 15° 29

4.5. Actual vs approximated radiated pattern--maximum phase error = 30° 30

4.6. Actual vs approximated radiated pattern--maximum phase error = 60° 30

FIGURE PAGE

4.7. Actual vs approximated radiated pattern--maximum phase error = 90° 31

4.8. Actual vs approximated radiated pattern--maximum phase error = 180° 31

LIST OF TABLES

TABLE PAGE

3.1. Actual gain vs approximated gain--
$a/\lambda = 0.5$, $b/\lambda = 2$, $\alpha = 1$ to $20°$ 13

3.2. Actual gain vs approximated gain--
$a/\lambda = 0.5$, $\beta/\lambda = 3$, $\alpha = 1$ to $20°$ 14

3.3. Actual gain vs approximated gain--
$a/\lambda = 0.5$, $\alpha = 2°$, $b/\lambda = 0.5$ to 6.0 15

3.4. Actual gain vs approximated gain--
$a/\lambda = 0.5$, $\alpha = 5°$, $b/\lambda = 0.5$ to 6.0 15

3.5. Actual gain vs approximated gain--
$a/\lambda = 0.5$, $\alpha = 10°$, $b/\lambda = 0.5$ to 6.0 16

3.6. Actual gain vs approximated gain--
$a/\lambda = 0.5$, $\alpha = 15°$, $b/\lambda = 0.5$ to 6.0 16

4.1. Actual vs approximated radiated pattern--
maximum phase error = 0° 23

4.2. Actual vs approximated radiated pattern--
maximum phase error = 15° 24

4.3. Actual vs approximated radiated pattern--
maximum phase error = 30° 25

4.4. Actual vs approximated radiated pattern--
maximum phase error = 60° 26

4.5. Actual vs approximated radiated pattern--
maximum phase error = 90° 27

4.6. Actual vs approximated radiated pattern--
maximum phase error=180° 28

LIST OF SYMBOLS AND ABBREVIATIONS

α - flare angle

δ - phase error

η - intrinsic impedance

λ - wavelength

μ - argument of Fresnel integral

$\theta, \theta', \theta''$ - angle of direction

a - horizontal antenna dimension

b - vertical antenna

C() - Fresnel integral cosine term

d - dimension of wave front approximation

dB - decibel

E - electric

E_E - electric field in E-plane

E_I - isotropic electric field

F() - Fresnel integral

G - calculated gain

G′ - approximated gain

GHz - GigaHertz

H - magnetic

H_E - magnetic field in E-plane

K - phase constant

ℓ - length

P_{ave} - average power density

P_{DE} - power density of E-plane antenna

(Continued)

P_{DI} - Power density of isotropic antenna

P_E - power radiated by E-plane antenna

P_I - power radiated by isotropic antenna

P_{max} - maximum power density

P_{total} - total radiated power

r - distance

S - area of aperture

S() - Fresnel integral sine term

1. INTRODUCTION

1.1 OBJECTIVE

The objective was to derive a gain and electric (E) field radiation pattern approximation for the E-plane horn antenna that could be used to avoid the complex mathematics and computation methods typically involved in calculating the gain and radiation pattern. Of course, as with other engineering approximations, there are limitations to their use that have to be recognized. The gain and E field radiation pattern of the E-plane horn antenna are a function of its physical dimensions, and these will govern the limitations of the approximations. The criterion used to evaluate the approximations was that the approximated values fall within 3 dB of the calculated values.

1.2 BACKGROUND

In general, the electromagnetic horn antenna is a simple aperture antenna used to provide a smooth transition for a wave traveling from a waveguide into free space. The dimensions of the waveguide are usually chosen to allow the propagation of one dominant mode, and the horn antenna will support only that mode by acting as a filter for other modes that might be excited in the transition. The horn antenna is popular in the microwave frequency range above 1 GHz and has the advantages of high gain, relatively wide bandwidth, and easy construction. However, a disadvantage is that the calculations for determining the gain and radiation patterns are mathematically rigorous and involve solving the Fresnel integral and performing numerical integration that may require using a computer.

1.3 DESCRIPTION OF E-PLANE HORN ANTENNA

The E-plane horn antenna is one of the basic types of horn antennas and is shown in Fig. 1.1. It is formed by flaring the waveguide in the E-plane, the y-z plane of the antenna's aperture. The horizontal dimension of the aperture is the same as the width of the original waveguide, and the vertical dimension is much greater than the height of the original waveguide.

A closer look at the E field and the magnetic (H) field in the E-plane horn antenna is shown in Fig. 1.2. The wave front is cylindrical, and the fields across the aperture are essentially an expanded version of the waveguide fields.

ORNL-DWG 88Z-8475

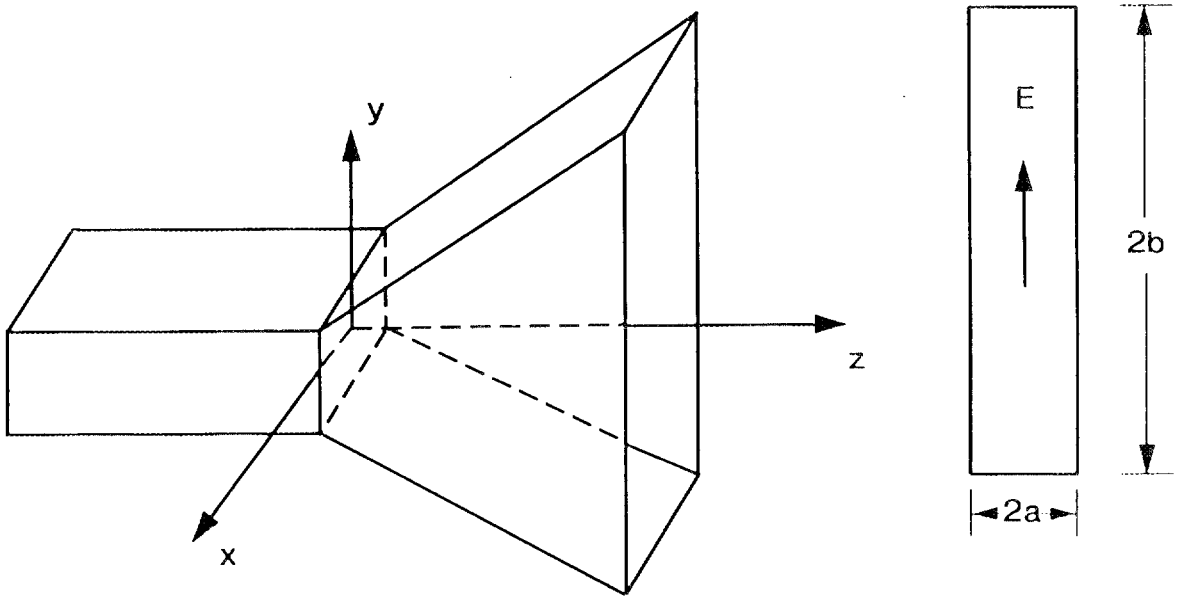

Fig. 1.1.The E-plane horn antenna.

ORNL-DWG 88Z-8474

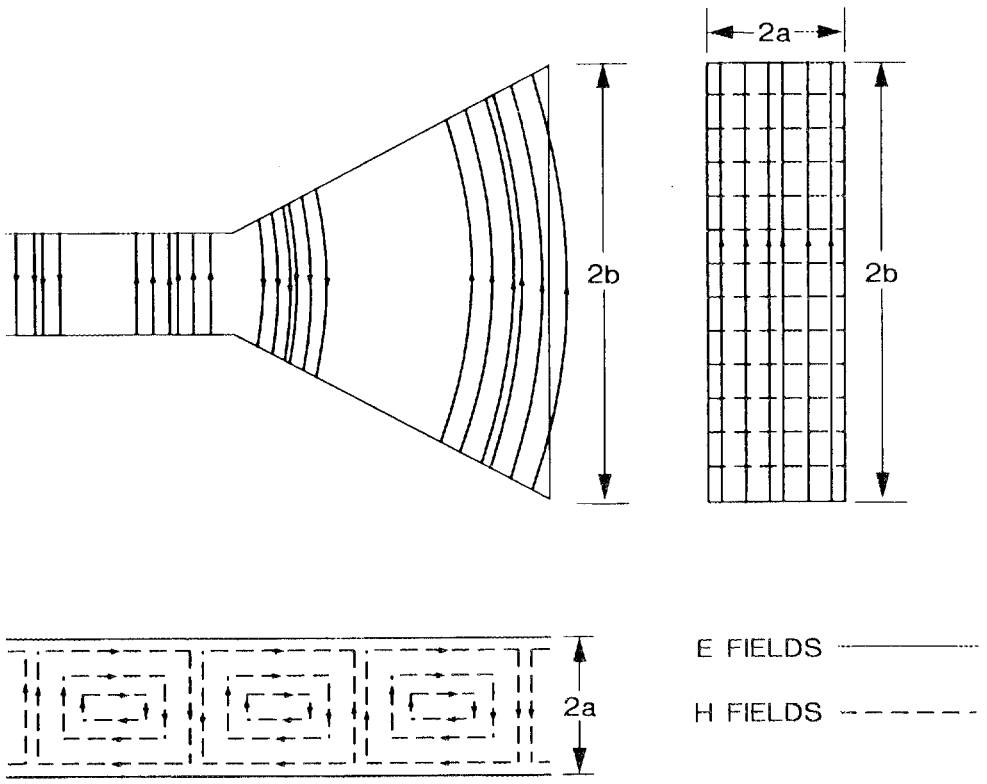

Fig. 1.2. E and H fields in the E-plane horn antenna.

2. GAIN AND RADIATION PATTERNS

2.1 APERTURE DISTRIBUTION

Knowledge of electromagnetic horn antenna theory has been around since the 1930s, and derivations of the gain and radiation patterns of the E-plane horn antenna are well documented.[1,2,3,4] The geometry of the E-plane horn antenna in the direction of the vertical flare is shown in Fig. 2.1. With the flare, the waves do not arrive at all points in the aperture at the same time, and therefore they form a cylindrical wave front with a phase error.

In Fig. 2.1, the length of the antenna flare and the angle of the flare are represented by ℓ and α, respectively. The phase error is represented by $\delta(Y_s)$, since it varies along the y axis, and can be expressed as

$$\delta(Y_s) = \frac{KY_s^2}{2\ell} \quad , \tag{2.1}$$

where the phase constant is a function of wavelength, λ, and is expressed as

$$K = \frac{2\pi}{\lambda} \quad . \tag{2.2}$$

The aperture distribution for the E-plane horn antenna is

$$E_s(Y_s) = E_o \, e^{-j\delta(Y_s)} \tag{2.3}$$

and, by substituting Eq. (2.1) into Eq. (2.3), can be expressed as

$$E_s(Y_s) = E_o \, e^{-jKY_s^2/2\ell} \quad , \tag{2.4}$$

where E_o is the distribution across a uniformly illuminated aperture.

2.2 GAIN

Antenna gain is the ratio of the maximum power density and the average power density in an antenna; that is,

$$G = P_{max}/P_{ave} \quad . \tag{2.5}$$

The maximum power density is

ORNL-DWG 88Z-8476

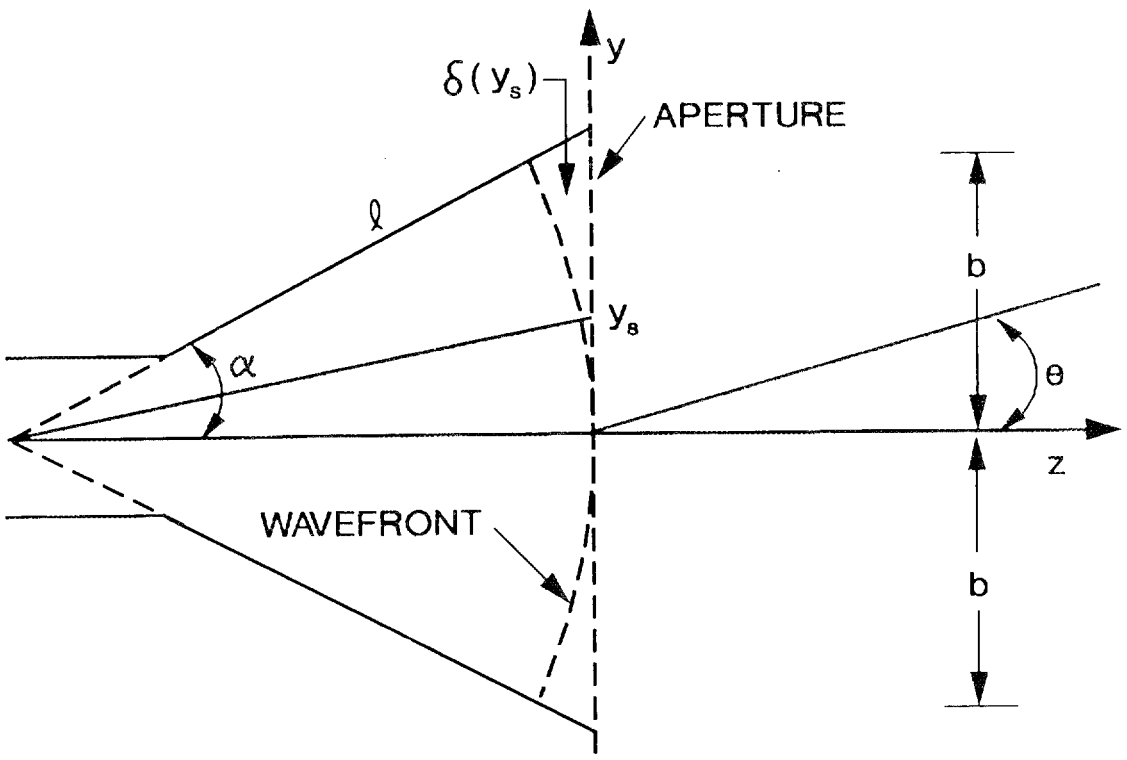

Fig. 2.1. Geometry of E-plane horn antenna.

$$P_{max} = \frac{1}{\eta r^2 \lambda^2} \left| \iint_S E_S(X_S, Y_S) dS \right|^2 \quad , \tag{2.6}$$

where the area of the aperture is designated as S with a differential area element dS, η is the intrinsic impedance of the medium, and r is the spherical coordinate indicating the distance to the point of observation. The average power density is the total radiated power for the area of a sphere, $4\pi r^2$. The total radiated power and the average power density can be expressed as

$$P_{total} = \iint_S \frac{|E_S(X_S, Y_S)|^2}{\eta} dS \tag{2.7}$$

and

$$P_{ave} = \iint_S \frac{|E_S(X_S, Y_S)|^2}{\eta \; 4\pi r^2} dS \quad . \tag{2.8}$$

The terms in Eq. (2.5) can be replaced by Eqs. (2.6) and (2.8) so that the gain becomes

$$G = \frac{4\pi}{\lambda^2} \frac{\left|\iint_S E_S(X_S,Y_S)\ dS\right|^2}{\iint_S \left|E_S(X_S,Y_S)\right|^2} dS \quad . \tag{2.9}$$

For the aperture distribution of the E-plane horn antenna given in Eq. (2.4) and the phase constant in Eq. (2.2), the gain is calculated to be

$$G = \frac{8\pi a\ell}{\lambda b} \left[C^2(\mu) + S^2(\mu)\right] \quad , \tag{2.10}$$

where

$$\mu = \sqrt{\frac{2}{\lambda\ell}}\ b \tag{2.11}$$

and $C(\mu)$ and $S(\mu)$ are Fresnel integrals. Another way of expressing the gain is with dimensions given in terms of the wavelength, and Eq. (2.10) thus becomes

$$G = 8\pi \frac{a/\lambda\ \ \ell/\lambda}{b/\lambda} \left[C^2(\mu) + S^2(\mu)\right] \quad . \tag{2.12}$$

2.3 RADIATION PATTERNS

The radiation patterns represent the radiating properties in the far field of an antenna and are a function of the direction from the antenna. They are the relative intensities of the E and H fields normalized to their maximum intensities.

The E field in the E-plane of a rectangular aperture is

$$E_E = j\ \frac{e^{-jKr}}{\lambda r} \cos^2 \frac{\Theta}{2} \iint_S E_S(X_S,Y_S)\ e^{jK\sin\Theta Y_S}\ dS \quad . \tag{2.13}$$

For the aperture distribution given in Eq. (2.4), Eq. (2.13) can be expressed as

$$E_E = jE_o\ \frac{e^{-jKr}}{\lambda r} \cos^2 \frac{\Theta}{2}\ 2a \int_{-b}^{b} e^{jK(\sin\Theta Y_S\ -\ Y_S^2/2\ell)}\ dY_S \quad . \tag{2.14}$$

The integral in Eq. (2.14) has no closed form and has to be evaluated by numerical means. Using numerical integration, the integral will take the form of

$$\int_{-b}^{b} e^{jK(\sin\theta Y_s - Y_s^2/2\ell)}\, dY_s = 2b\ F(Kb\sin\theta,\delta) \quad , \tag{2.15}$$

where $F(Kb\sin\theta,\delta)$ is the relative E field radiation pattern for the E-plane horn antenna. A graphical representation of $F(Kb\sin\theta,\delta)$, as a function of phase error and the direction from the antenna, is shown in Fig. 2.2.

The H field in the E-plane of a rectangular aperture is

$$H_E = j\ \frac{e^{-jKr}}{\lambda r} \cos^2 \frac{\theta}{2} \iint_S E_s(X_s,Y_s)\ e^{jK\sin\theta X_s}\, dS \quad . \tag{2.16}$$

By substituting the aperture distribution in Eq. (2.4), the H field can be expressed as

$$H_E = j\ \frac{2}{\pi}\ E_o\ \frac{e^{-jKr}}{\lambda r} \cos^2 \frac{\theta}{2}\ \ 4ab\ \frac{C(\mu)\ -jS(\mu)}{\mu}\ \frac{\cos(Ka\sin\theta)}{1\ -\ (\frac{2}{\pi}\ Ka\sin\theta)^2} \quad , \tag{2.17}$$

where

$$\mu = \sqrt{\frac{2}{\lambda\ell}}\ b \quad .$$

Thus, the relative H field pattern is

$$F(Ka\sin\theta) = \frac{\cos(Ka\sin\theta)}{1\ -\ (\frac{2}{\pi}\ Ka\sin\theta)^2} \quad . \tag{2.18}$$

Figure 2.3 is a graphical representation of the relative H field radiation pattern as a function of the direction from the antenna.

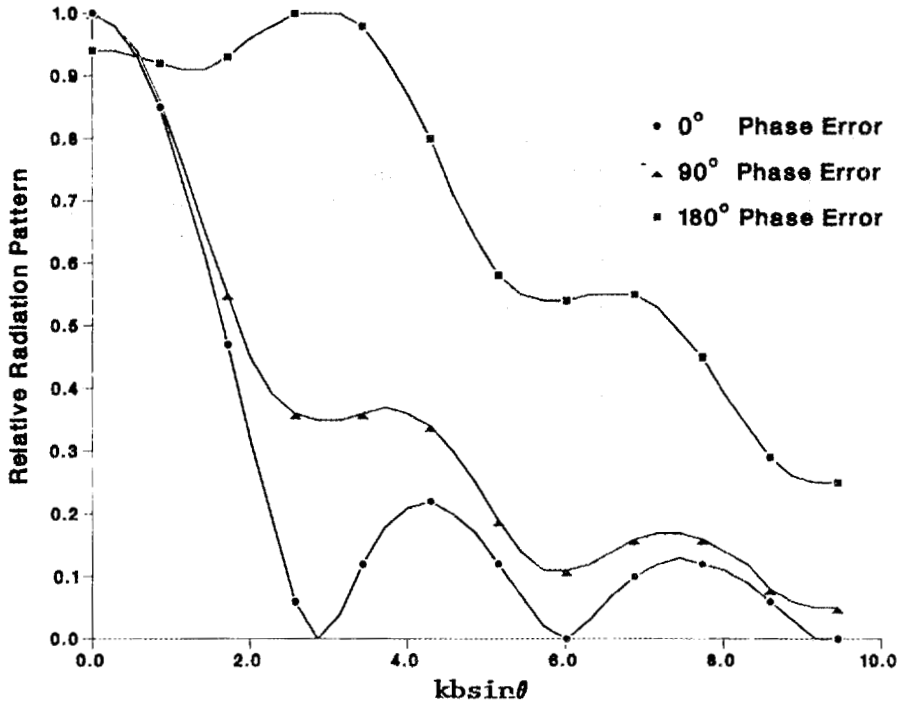

Fig. 2.2. Relative E field radiation pattern.

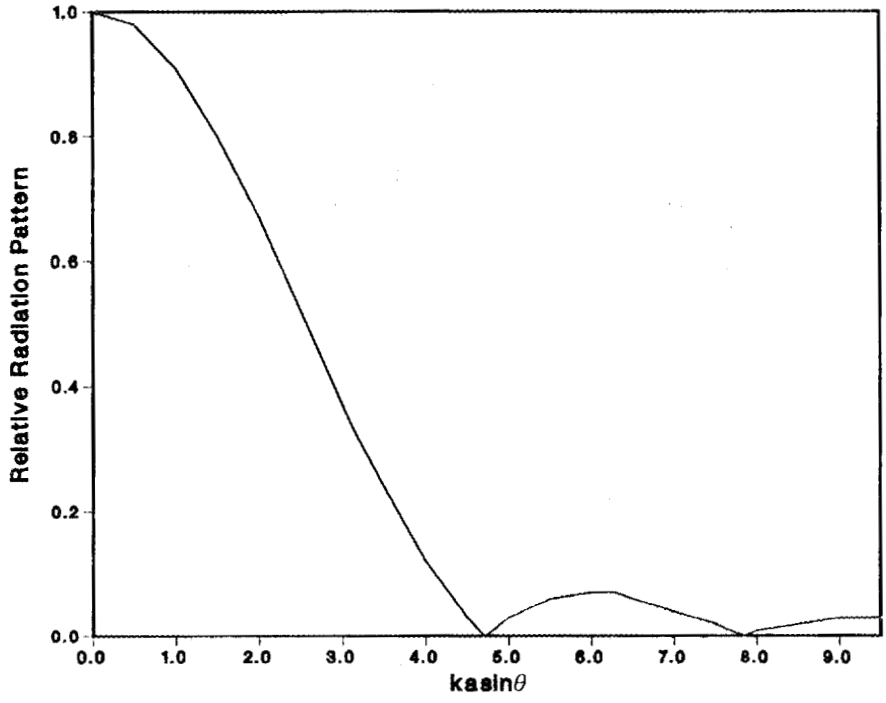

Fig. 2.3. Relative H field radiation pattern.

3. GAIN APPROXIMATION

3.1 ACTUAL GAIN

Gain is the increase in the power radiated by the E-plane horn antenna in a given direction over the power radiated by a lossless isotropic antenna emitting the same total power. It is expressed as the ratio of the maximum power density and the average power density and is independent of the actual power levels. The gain of the E-plane horn antenna was derived in Sect. 2, where it was expressed as

$$G = 8\pi \frac{a/\lambda \ \ell/\lambda}{b/\lambda} \left[C^2(\mu) + S^2(\mu)\right] \quad , \tag{2.12}$$

with

$$\mu = \sqrt{\frac{2}{\lambda \ell}}\, b \quad . \tag{2.11}$$

3.2 APPROACH TO GAIN APPROXIMATION

An approach to approximating the gain can be the ratio of the power radiated by the E-plane horn antenna (P_E) to the power radiated by a lossless isotropic antenna (P_I); that is,

$$G' = \frac{P_I}{P_E} \quad , \tag{3.1}$$

with a linear approximation of the E-plane horn antenna wave front being used to estimate P_E. The ratio of P_I and P_E can be derived by letting the magnitude of the E field strength from the isotropic antenna (E_I) equal the magnitude of the E field strength from the E-plane horn antenna (E_E); that is,

$$\left| E_I \right| = \left| E_E \right| \quad . \tag{3.2}$$

3.3 MAGNITUDE OF E FIELD FROM ISOTROPIC ANTENNA

For the isotropic antenna, the power density (P_{DI}) can be used to relate P_I and E_I since

$$P_{DI} = \frac{E_I^2}{\eta} \tag{3.3}$$

and

$$P_{DI} = \frac{P_I}{4\pi r^2} \quad . \tag{3.4}$$

By setting the power density terms equal,

$$\frac{E_I^2}{\eta} = \frac{P_I}{4\pi r^2} \quad , \tag{3.5}$$

and E_I can be expressed as

$$E_I = \sqrt{\frac{\eta \ P_I}{4\pi r^2}} \quad . \tag{3.6}$$

If the intrinsic impedance is replaced by $\eta = 120\pi = 377$ for the far field,

$$E_I = \frac{\sqrt{30 \ P_I}}{r} \quad . \tag{3.7}$$

The E field radiation pattern for an isotropic antenna is also isotropic, so

$$\left| \ E_I \ \right| = \frac{\sqrt{30 \ P_I}}{r} \quad . \tag{3.8}$$

3.4 LINEAR APPROXIMATION OF WAVE FRONT FROM E-PLANE HORN ANTENNA

Figure 3.1 shows a linear approximation of the E-plane horn antenna wave front. The linear approximation will divide the wave front and the antenna into two sections with each acting as an independent horn antenna. With the linear approximation, the vertical dimension b can be replaced by

$$d = \frac{b}{\cos\alpha} \quad . \tag{3.9}$$

The phase error is zero, and the angular direction away from the antenna is approximately the angle of the antenna flare.

ORNL-DWG 86Z-8477

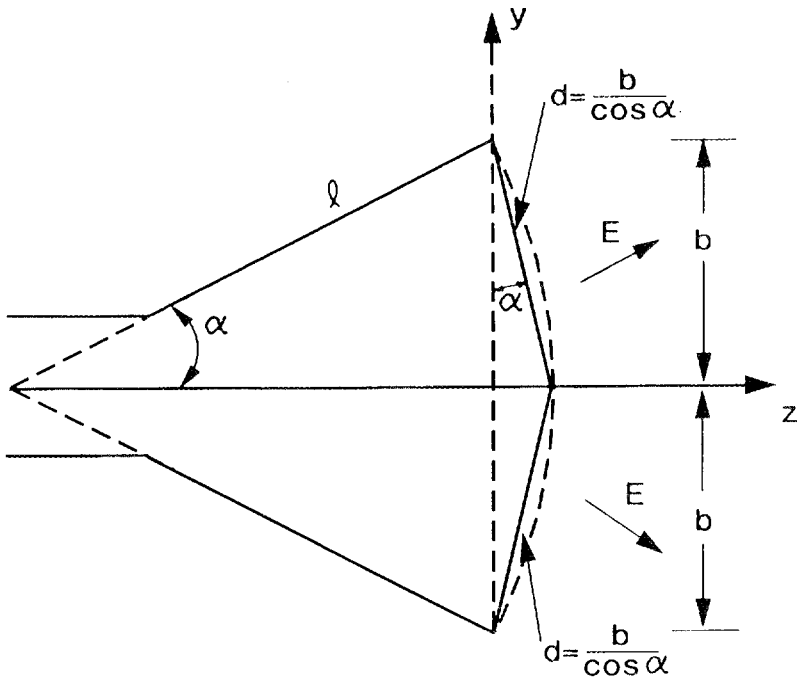

Fig. 3.1. Geometry of linear approximation.

3.5 MAGNITUDE OF E FIELD FROM E-PLANE HORN ANTENNA

The E field at the aperture opening was given in Sect. 2 and was expressed as

$$E_E = j \frac{e^{-jKr}}{\lambda r} \cos^2 \frac{\theta}{2} \iint_S E_S(X_S, Y_S)\, e^{jK\sin\theta Y_S}\, dS \quad . \tag{2.13}$$

With the linear approximation, the aperture distribution is

$$E_S(X_S, Y_S) = E_o \quad , \tag{3.10}$$

and the E field is

$$E_E = 2j \frac{e^{-jKr}}{\lambda r} \cos^2 \frac{\alpha}{2} E_o \int_{-a}^{a} dX_S \int_{-d/2}^{d/2} e^{jK\sin\alpha Y_S}\, dY_S \quad . \tag{3.11}$$

By solving the integrals in Eq. (3.11), the E field can be expressed as

$$E_E = 2j \frac{e^{-jKr}}{\lambda r} \cos^2 \frac{\alpha}{2} E_o \, 2a \left[\frac{d \sin(K\, d/2 \sin\alpha)}{K\, d/2 \sin\alpha}\right] . \tag{3.12}$$

Also, if the d term is replaced by its value in Eq. (3.9), the E field becomes

$$E_E = 2j \frac{e^{-jKr}}{\lambda r} \cos^2 \frac{\alpha}{2} E_o \frac{2ab}{\cos\alpha} \left[\frac{\sin\left(K \frac{b}{2\cos\alpha} \sin\alpha\right)}{K \frac{b}{2\cos\alpha} \sin\alpha}\right] \tag{3.13}$$

or

$$E_E = 2j \frac{e^{-jKr}}{\lambda r} \cos^2 \frac{\alpha}{2} E_o \frac{2ab}{\cos\alpha} \left[\frac{\sin(K\, b/2 \tan\alpha)}{K\, b/2 \tan\alpha}\right] . \tag{3.14}$$

So, from the E field in Eq. (3.14), its magnitude can be expressed as

$$\left|E_E\right| = \frac{4ab}{\lambda r \cos\alpha} E_o \cos^2 \frac{\alpha}{2} \left[\frac{\sin(K\, b/2 \tan\alpha)}{K\, b/2 \tan\alpha}\right] . \tag{3.15}$$

However, the magnitude of E_E is not expressed in terms of P_E, and the power density of one section of the antenna (P_{DE}) will have to be used to relate E_E and P_E; that is,

$$P_{DE} = \frac{E_o^2}{\eta} , \tag{3.16}$$

and

$$P_{DE} = \frac{P_E/2}{2ab/\cos\alpha} . \tag{3.17}$$

By setting the power density terms equal,

$$\frac{E_o^2}{\eta} = \frac{P_E/2}{2ab/\cos\alpha} , \tag{3.18}$$

and the uniformly illuminated aperture distribution is

$$E_o = \sqrt{\frac{\eta\, P_E/2 \cos\alpha}{2ab}} . \tag{3.19}$$

If the intrinsic impedance $\eta = 120\pi = 377$ is substituted,

$$E_o = \sqrt{\frac{60\pi\ P_E\ \cos\alpha}{2ab}} \quad . \tag{3.20}$$

Subsequently, the substitution of Eq. (3.20) into Eq. (3.15) will yield

$$\left|E_E\right| = \frac{4ab}{\lambda r\ \cos\alpha}\ \frac{60\pi\ P_E\ \cos\alpha}{2ab}\ \cos^2\frac{\alpha}{2}\left[\frac{\sin(K\ b/2\ \tan\alpha)}{K\ b/2\ \tan\alpha}\right] \quad . \tag{3.21}$$

3.6 GAIN APPROXIMATION USING E FIELD MAGNITUDES

With the magnitude of the E field from the E-plane horn antenna in Eq. (3.21) and the magnitude of the E field from the lossless isotropic antenna in Eq. (3.8), the equality set forth in Eq. (3.2) can be completed and will yield

$$\frac{30\ P_I}{r} = \frac{4ab}{\lambda r\ \cos\alpha}\ \frac{60\pi\ P_E\ \cos\alpha}{2ab}\ \cos^2\frac{\alpha}{2}\left[\frac{\sin(K\ b/2\ \tan\alpha)}{K\ b/2\ \tan\alpha}\right] \quad . \tag{3.22}$$

By squaring both sides of Eq. (3.22), manipulating the terms, and substituting the value of the phase constant K, the ratio of P_I and P_E and in turn the approximated gain becomes

$$G' = \frac{P_I}{P_E} = 16\pi\ a/\lambda\ b/\lambda\ \frac{\cos^4\ \alpha/2}{\cos\alpha}\left[\frac{\sin(\pi\ b/\lambda\ \tan\alpha)}{\pi\ b/\lambda\ \tan\alpha}\right]^2 \quad . \tag{3.23}$$

3.7 COMPARISON OF ACTUAL GAIN AND APPROXIMATED GAIN

Comparisons of the actual gain and the derived gain approximation are shown on subsequent pages for variations in the b/λ and α dimensions of the antenna. More specifically, comparisons of the gains are shown where the flare angle α is varying with a horizontal aperture dimension of $a/\lambda = 0.5$ and a vertical aperture dimension of $b/\lambda = 2$ and $b/\lambda = 3$, respectively. It should also be kept in mind that a variation in the flare angle will also mean a variation in the length ℓ of the antenna. Also, comparisons are shown where the vertical aperture dimension b/λ is varying with the same horizontal aperture dimension of $a/\lambda = 0.5$ and an angle flare of $\alpha = 2°$, $\alpha = 5°$, $\alpha = 10°$, and $\alpha = 15°$ respectively. Tables 3.1 through 3.6 show the comparisons in a tabular form, and Fig. 3.2 through 3.7 illustrate the corresponding graphical representations.

Table 3.1. Actual gain vs approximated gain--
$a/\lambda = 0.5$, $b/\lambda = 2$, $\alpha = 1$ to 20°

α(°)	G	G(dB)	G′	G′(dB)	G′/G	G′/G(dB)
1	50.19	17.01	50.06	16.99	0.998	-0.02
2	50.01	16.99	49.46	16.94	0.989	-0.05
3	49.70	16.96	48.47	16.85	0.975	-0.11
4	49.31	16.93	47.10	16.73	0.955	-0.20
5	48.90	16.89	45.38	16.57	0.928	-0.32
6	48.19	16.83	43.34	16.37	0.899	-0.46
7	47.68	16.78	41.01	16.13	0.860	-0.65
8	46.72	16.70	38.43	15.85	0.823	-0.85
9	46.02	16.63	35.65	15.52	0.775	-1.11
10	44.92	16.52	32.71	15.15	0.728	-1.37
11	43.97	16.43	29.66	14.72	0.675	-1.71
12	42.94	16.33	26.55	14.24	0.618	-2.09
13	41.66	16.20	23.44	13.70	0.563	-2.50
14	40.62	16.09	20.37	13.09	0.502	-3.00
15	39.33	15.95	17.40	12.41	0.442	-3.54
16	37.94	15.79	14.56	11.63	0.384	-4.16
17	36.77	15.65	11.91	10.76	0.324	-4.89
18	35.45	15.50	9.47	9.76	0.267	-5.74
19	33.93	15.31	7.29	8.63	0.215	-6.68
20	32.62	15.13	5.38	7.31	0.165	-7.82

Table 3.2. Actual gain vs approximated gain--
$a/\lambda = 0.5$, $b/\lambda = 3$, $\alpha = 1$ to 20°

α(°)	G	G(dB)	G'	G'(dB)	G'/G	G'/G(dB)
1	75.16	18.76	74.72	18.73	0.994	- 0.03
2	74.55	18.72	72.70	18.62	0.975	- 0.10
3	73.60	18.67	69.43	18.42	0.943	- 0.25
4	72.29	18.59	65.04	18.13	0.900	- 0.46
5	70.73	18.50	59.71	17.76	0.844	- 0.74
6	69.02	18.39	53.65	17.30	0.777	- 1.09
7	66.57	18.23	47.08	16.73	0.707	- 1.50
8	64.31	18.08	40.28	16.05	0.626	- 2.03
9	61.56	17.89	33.47	15.25	0.544	- 2.64
10	58.77	17.69	26.91	14.30	0.458	- 3.39
11	55.76	17.46	20.80	13.18	0.373	- 4.28
12	52.75	17.22	15.32	11.85	0.290	- 5.37
13	49.45	16.94	10.63	10.27	0.215	- 6.67
14	46.55	16.68	6.79	8.32	0.146	- 8.36
15	42.99	16.33	3.85	5.85	0.090	-10.48
16	40.03	16.02	1.80	2.55	0.045	-13.47
17	36.75	15.65	0.56	- 2.52	0.015	-18.17
18	33.63	15.27	0.04	-14.01	0.001	-29.28
19	30.97	14.91	0.09	-10.46	0.003	-25.37
20	27.88	14.45	0.55	- 2.60	0.020	-17.05

Table 3.3. Actual gain vs approximated gain--
$a/\lambda = 0.5$, $\alpha = 2°$, $b/\lambda = 0.5$ to 6.0

b/λ	G	G(dB)	G'	G'(dB)	G'/G	G'/G(dB)
0.5	12.56	10.99	12.55	10.99	0.999	-0.00
1.0	25.09	14.00	25.03	13.98	0.998	-0.02
1.5	37.58	15.75	37.36	15.72	0.994	-0.03
2.0	50.01	16.99	49.46	16.94	0.989	-0.05
2.5	62.35	17.95	61.26	17.87	0.983	-0.08
3.0	74.55	18.72	72.70	18.62	0.975	-0.10
3.5	86.79	19.38	83.70	19.23	0.964	-0.15
4.0	98.61	19.94	94.21	19.74	0.955	-0.20
4.5	110.40	20.43	104.16	20.18	0.943	-0.25
5.0	122.24	20.87	113.49	20.55	0.928	-0.32
5.5	133.49	21.25	122.17	20.87	0.915	-0.38
6.0	144.56	21.60	130.13	21.14	0.900	-0.46

Table 3.4. Actual gain vs approximated gain--
$a/\lambda = 0.5$, $\alpha = 5°$, $b/\lambda = 0.5$ to 6.0

b/λ	G	G(dB)	G'	G'(dB)	G'/G	G'/G(dB)
0.5	12.54	10.98	12.49	10.97	0.995	-0.01
1.0	24.94	13.97	24.50	13.89	0.983	-0.08
1.5	37.09	15.69	35.60	15.51	0.960	-0.18
2.0	48.90	16.89	45.38	16.57	0.928	-0.32
2.5	60.05	17.79	53.50	17.28	0.891	-0.51
3.0	70.73	18.50	59.71	17.76	0.844	-0.74
3.5	80.78	19.07	63.85	18.05	0.790	-1.02
4.0	89.76	19.53	65.86	18.19	0.734	-1.34
4.5	98.36	19.93	65.78	18.18	0.669	-1.75
5.0	105.39	20.23	63.75	18.04	0.605	-2.19
5.5	112.05	20.49	59.98	17.78	0.535	-2.71
6.0	117.27	20.69	54.77	17.39	0.467	-3.30

Table 3.5. Actual gain vs approximated gain--
$a/\lambda = 0.5$, $\alpha = 10°$, $b/\lambda = 0.5$ to 6.0

b/λ	G	G(dB)	G'	G'(dB)	G'/G	G'/G(dB)
0.5	12.47	10.96	12.25	10.88	0.982	- 0.08
1.0	24.45	13.88	22.65	13.55	0.926	- 0.33
1.5	35.39	15.49	29.75	14.73	0.841	- 0.76
2.0	44.92	16.52	32.71	15.15	0.728	- 1.37
2.5	52.77	17.22	31.52	14.99	0.597	- 2.23
3.0	58.77	17.69	26.91	14.30	0.458	- 3.39
3.5	62.94	17.99	20.18	13.05	0.321	- 4.94
4.0	64.46	18.09	12.89	11.10	0.200	- 6.99
4.5	64.00	18.06	6.49	8.12	0.101	- 9.94
5.0	62.26	17.94	2.07	3.16	0.033	-14.78
5.5	58.81	17.69	0.11	-9.59	0.002	-27.28
6.0	53.95	17.32	0.49	-3.10	0.009	-20.42

Table 3.6. Actual gain vs approximated gain--
$a/\lambda = 0.5$, $\alpha = 15$, $b/\lambda = 0.5$ to 6.0

b/λ	G	(dB)	G'	G'(dB)	G'/G	G'/G(dB)
0.5	12.37	10.92	11.84	10.73	0.957	- 0.19
1.0	23.61	13.73	19.71	12.95	0.835	- 0.78
1.5	32.86	15.17	21.41	13.31	0.651	- 1.86
2.0	39.33	15.95	17.40	12.41	0.442	- 3.54
2.5	42.63	16.30	10.39	10.17	0.244	- 6.13
3.0	42.99	16.33	3.85	5.86	0.090	-10.47
3.5	40.71	16.10	0.35	-4.56	0.009	-20.66
4.0	36.47	15.62	0.48	-3.19	0.013	-18.81
4.5	31.11	14.93	2.92	4.65	0.094	-10.28
5.0	25.48	14.06	5.48	7.39	0.215	- 6.67
5.5	20.33	13.08	6.38	8.05	0.314	- 5.03
6.0	16.70	12.23	5.18	7.14	0.310	- 5.09

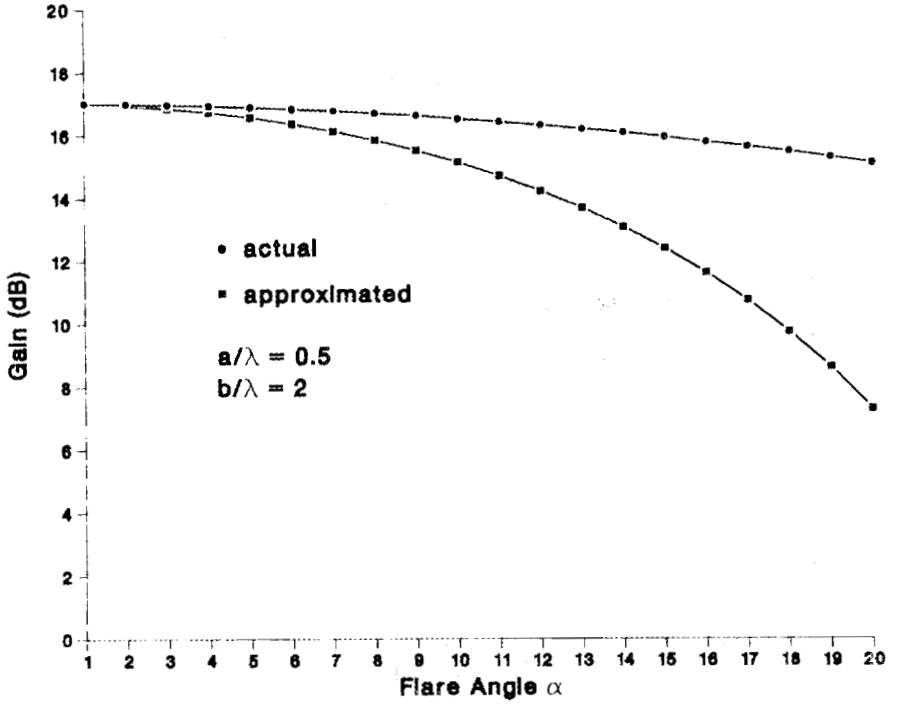

Fig. 3.2. Actual gain vs approximated gain--
$a/\lambda = 0.5$, $b/\lambda = 2$, $\alpha = 1$ to $20°$.

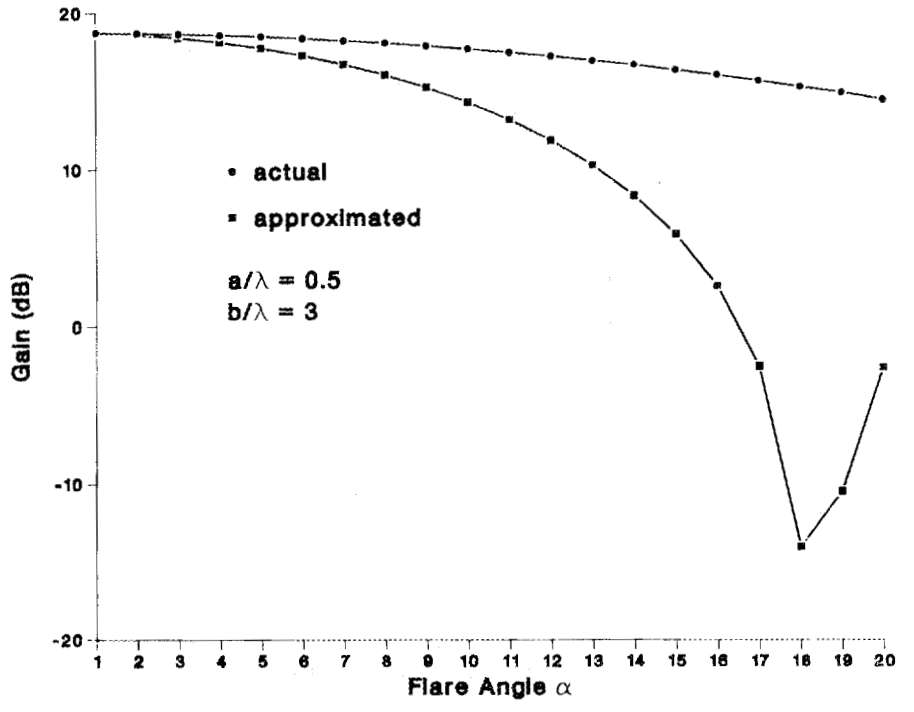

Fig. 3.3. Actual gain vs approximated gain--
$a/\lambda = 0.5$, $b/\lambda = 3$, $\alpha = 1$ to $20°$.

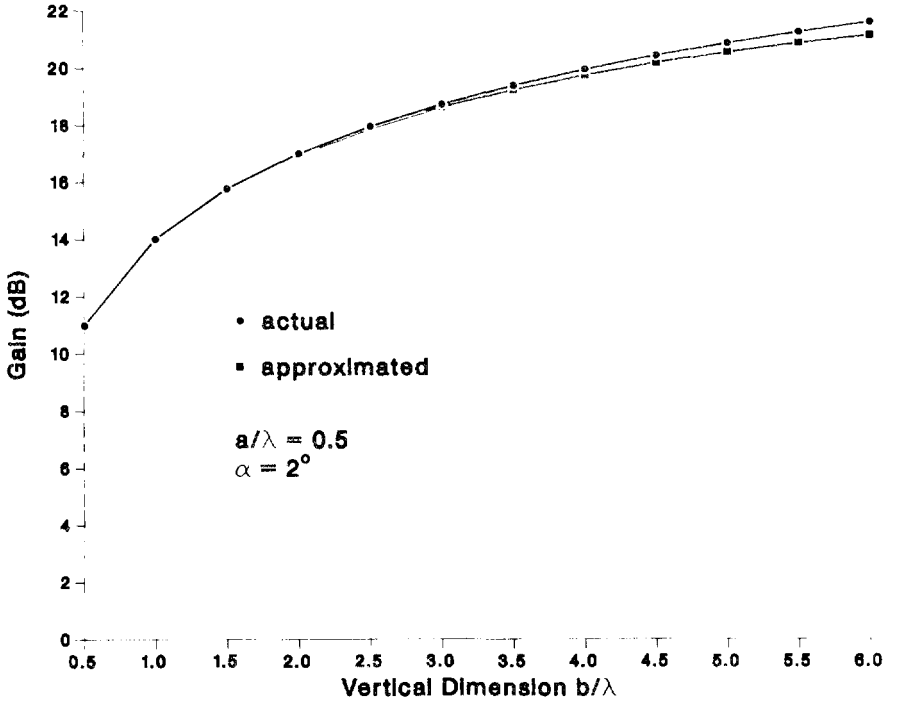

Fig. 3.4. Actual gain vs approximated gain--
$a/\lambda = 0.5$, $\alpha = 2°$, $b/\lambda = 0.5$ to 6.0.

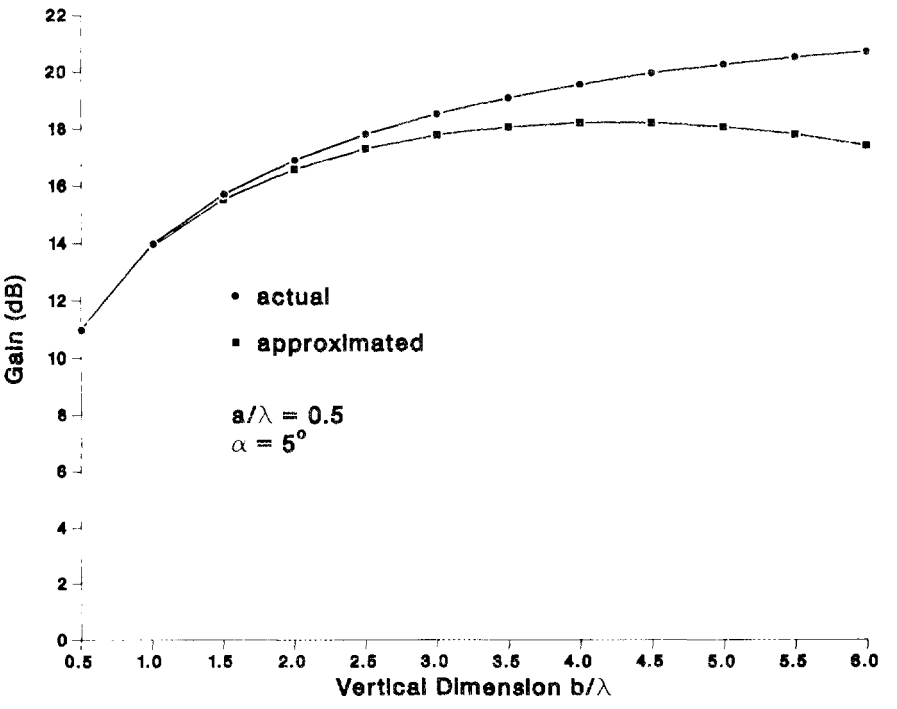

Fig. 3.5. Actual gain vs approximated gain--
$a/\lambda = 0.5$, $\alpha = 5°$, $b/\lambda = 0.5$ to 6.0.

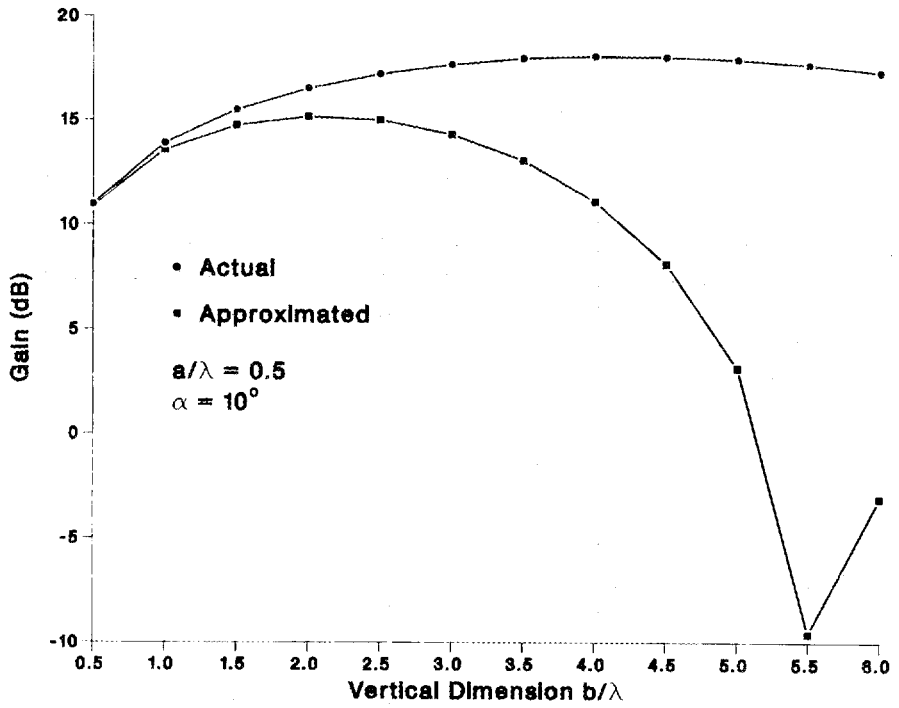

Fig. 3.6. Actual gain vs approximated gain--
$a/\lambda = 0.5$, $\alpha = 10°$, $b/\lambda = 0.5$ to 6.0.

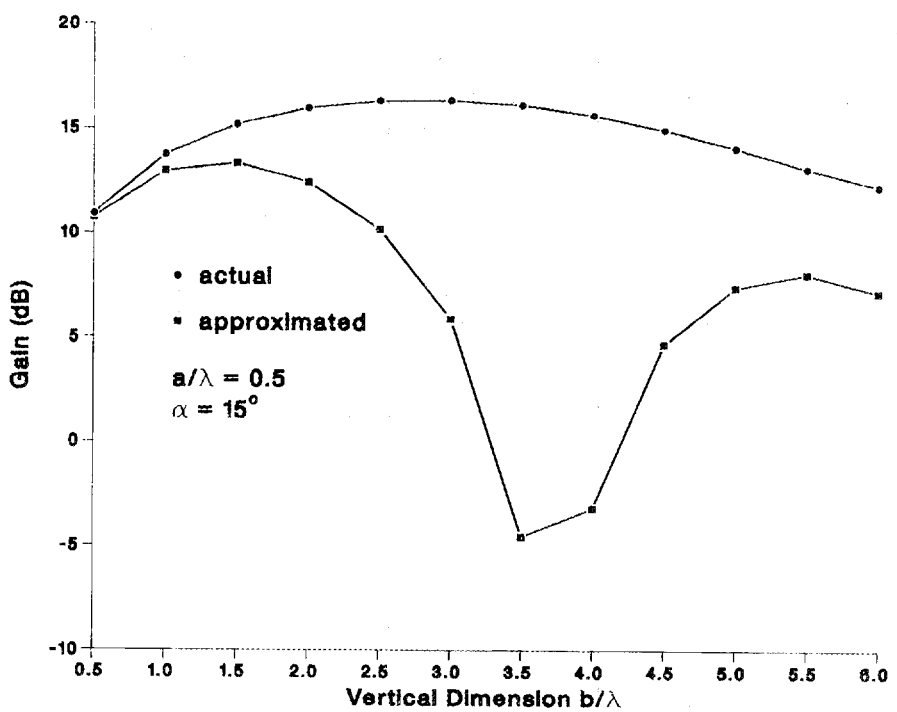

Fig. 3.7. Actual gain vs approximated gain--
$a/\lambda = 0.5$, $\alpha = 15°$, $b/\lambda = 0.5$ to 6.0.

4. RADIATION PATTERN APPROXIMATION

4.1 ACTUAL RADIATION PATTERN

As shown in Eq. (2.18), the H field radiation pattern in the E-plane is rather simple to calculate, making it unnecessary to use an approximation to derive it. However, the E field radiation pattern in the E-plane is more complex and requires the use of numerical integration for its evaluation. The actual E field radiation pattern can be expressed as

$$F(Kb\sin\theta,\delta) = \frac{1}{2b}\int_{-b}^{b} e^{jK(\sin\theta Y_s - Y_s^2/2\ell)}\, dY_s \quad . \tag{4.1}$$

The pattern of the E-plane horn antenna is shown in Fig. 4.1, and the relative E field radiation pattern, as a function of direction and phase error, has been previously shown in Fig. 2.2.

4.2 APPROACH TO RADIATION PATTERN APPROXIMATION

An approach to approximating the E field radiation pattern can be similar to the one used for the gain approximation in the sense that the antenna will again be divided into two sections with each acting as an independent antenna. Figure 4.2 shows the geometry of each section and its associated pattern. An estimate of the total radiation pattern will encompass a combination of the individual radiation patterns related by the angles of direction θ' and θ''.

4.3 APPROXIMATION OF E-PLANE RADIATION PATTERN

An approximation of the E-plane radiation pattern will involve the radiation patterns of the individual sections which can be expressed as

$$F(Kb\sin\theta') = \frac{\sin\,(Kb\sin\theta')}{Kb\sin\theta'} \tag{4.2}$$

and

$$F(Kb\sin\theta'') = \frac{\sin\,(Kb\sin\theta'')}{Kb\sin\theta''} \quad . \tag{4.3}$$

The radiation patterns in Eqs. (4.2) and (4.3) are the patterns for the E-plane radiation from a rectangular aperture. From Fig. 4.2, the angles θ' and θ'' are related to the original angle of direction θ and the flare angle α of the E-plane horn antenna by

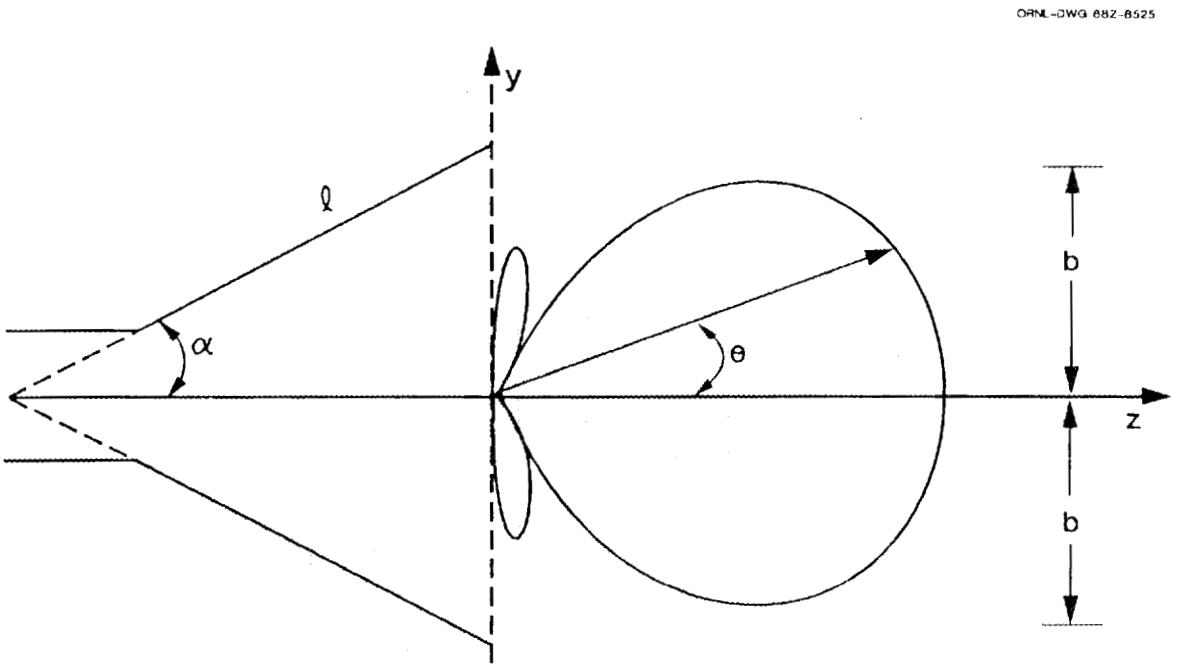

Fig. 4.1. E-plane horn antenna pattern.

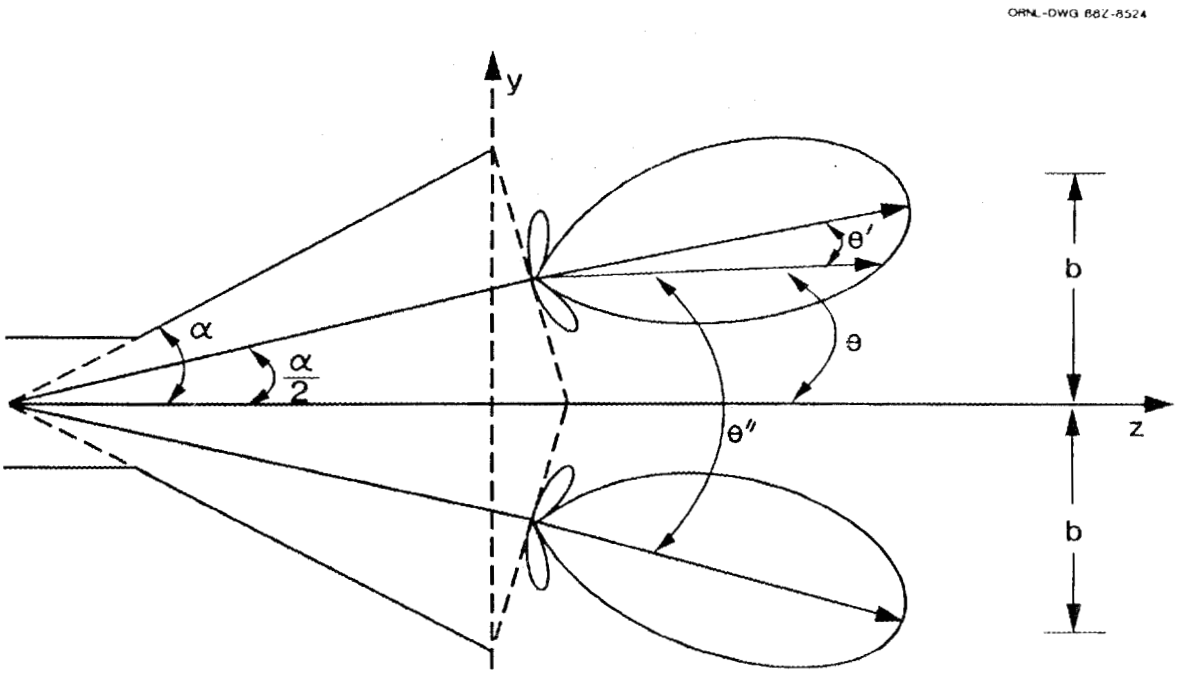

Fig. 4.2. Geometry of E-plane radiation pattern approximation.

$$\theta' = \frac{\alpha}{2} - \theta \tag{4.4}$$

and

$$\theta'' = \frac{\alpha}{2} + \theta \quad . \tag{4.5}$$

The E-plane radiation pattern approximation will combine Eqs. (4.2) and (4.3) and can be expressed as

$$F'(Kb\sin\theta) = \frac{1}{2}\left[\frac{\sin(Kb\sin\theta')}{Kb\sin\theta'} + \frac{\sin(Kb\sin\theta'')}{Kb\sin\theta''}\right] \quad . \tag{4.6}$$

The final expression in Eq. (4.6) is actually only half of the sum of the radiation patterns of the two sections because of the overlap between them.

4.4 COMPARISON OF ACTUAL AND APPROXIMATED RADIATION PATTERN

Comparisons of the actual E field radiation pattern and the approximated radiation pattern are shown in Tables 4.1 through 4.6 for various values of the maximum phase error. The actual and approximated radiation pattern values are specified as $F(Kb\sin\theta)$ and $F'(Kb\sin\theta)$, respectively. Figures 4.3 through 4.8 are the corresponding graphical representations of Tables 4.1 through 4.6.

Table 4.1. Actual vs approximated radiation pattern--maximum phase error = 0°

Kbsinθ	F(Kbsinθ)	F'(Kbsinθ)	Ratio	Ratio(dB)
0.000	1.000	1.000	1.000	0.000
0.330	0.982	0.982	1.000	0.000
0.660	0.929	0.929	1.000	0.000
0.989	0.845	0.845	1.000	0.000
1.318	0.734	0.734	1.000	0.000
1.647	0.605	0.605	1.000	0.000
1.976	0.465	0.465	1.000	0.001
2.303	0.323	0.323	1.000	0.001
2.630	0.186	0.186	1.000	0.001
2.957	0.062	0.062	1.000	0.001
3.141	0.000	0.000	1.000	0.000
3.282	0.043	0.043	1.000	0.001
3.606	0.124	0.124	1.000	0.002
3.929	0.180	0.180	1.001	0.002
4.251	0.211	0.211	1.001	0.003
4.572	0.216	0.217	1.001	0.003
4.981	0.201	0.201	1.001	0.003
5.209	0.169	0.169	1.001	0.004
5.525	0.124	0.124	1.001	0.004
5.840	0.073	0.073	1.001	0.005
6.153	0.021	0.021	1.001	0.005
6.283	0.000	0.000	1.000	0.000
6.463	0.028	0.028	1.001	0.006
6.772	0.069	0.069	1.002	0.007
7.079	0.101	0.101	1.002	0.007
7.384	0.121	0.121	1.002	0.008
7.686	0.128	0.128	1.002	0.009
7.986	0.124	0.124	1.002	0.009
8.284	0.109	0.110	1.002	0.010
8.579	0.087	0.087	1.002	0.011
8.871	0.059	0.059	1.003	0.011
9.161	0.028	0.028	1.003	0.012

Table 4.2. Actual vs approximated radiation pattern--maximum phase error = 15°

Kbsinθ	F(Kbsinθ)	F'(Kbsinθ)	Ratio	Ratio(dB)
0.000	0.997	0.989	0.992	0.037
0.330	0.979	0.971	0.992	0.036
0.660	0.926	0.919	0.992	0.034
0.989	0.842	0.836	0.993	0.031
1.318	0.733	0.728	0.994	0.026
1.647	0.605	0.602	0.996	0.019
1.976	0.466	0.465	0.997	0.012
2.303	0.325	0.325	0.998	0.009
2.630	0.192	0.190	0.989	0.050
2.957	0.082	0.068	0.837	0.773
3.282	0.068	0.035	0.519	2.852
3.606	0.134	0.116	0.866	0.624
3.929	0.186	0.172	0.925	0.338
4.251	0.214	0.203	0.946	0.239
4.572	0.219	0.210	0.958	0.189
4.891	0.203	0.196	0.965	0.156
5.209	0.170	0.165	0.970	0.132
5.525	0.126	0.122	0.975	0.112
5.840	0.075	0.073	0.976	0.104
6.153	0.025	0.022	0.887	0.520
6.463	0.031	0.025	0.825	0.834
6.772	0.071	0.066	0.937	0.284
7.079	0.102	0.097	0.956	0.197
7.384	0.121	0.117	0.964	0.161
7.686	0.129	0.125	0.968	0.140
7.986	0.124	0.121	0.972	0.124
8.284	0.110	0.107	0.975	0.110
8.579	0.087	0.086	0.978	0.096
8.871	0.060	0.058	0.981	0.083
9.161	0.029	0.028	0.979	0.093

Table 4.3. Actual vs approximated radiation pattern--maximum phase error = 30°

Kbsinθ	F(Kbsinθ)	F'(Kbsinθ)	Ratio	Ratio(dB)
0.000	0.988	0.955	0.967	0.148
0.330	0.970	0.938	0.967	0.145
0.660	0.918	0.890	0.969	0.137
0.989	0.836	0.812	0.972	0.124
1.318	0.728	0.711	0.976	0.104
1.647	0.602	0.592	0.982	0.079
1.976	0.467	0.462	0.989	0.050
2.303	0.333	0.330	0.991	0.038
2.630	0.210	0.202	0.962	0.167
2.957	0.122	0.086	0.703	1.530
3.282	0.114	0.014	0.119	9.260
3.606	0.160	0.092	0.576	2.394
3.929	0.203	0.148	0.730	1.366
4.251	0.226	0.180	0.798	0.981
4.572	0.227	0.190	0.836	0.779
4.891	0.209	0.180	0.861	0.648
5.209	0.174	0.154	0.881	0.549
5.525	0.129	0.116	0.898	0.467
5.840	0.079	0.072	0.906	0.430
6.153	0.035	0.025	0.730	1.364
6.463	0.039	0.019	0.479	3.194
6.772	0.075	0.057	0.760	1.194
7.079	0.105	0.086	0.824	0.840
7.384	0.124	0.105	0.853	0.691
7.686	0.131	0.114	0.870	0.602
7.986	0.126	0.111	0.884	0.537
8.284	0.111	0.100	0.895	0.481
8.579	0.089	0.080	0.906	0.427
8.871	0.061	0.056	0.918	0.374
9.161	0.031	0.028	0.913	0.398

Table 4.4. Actual vs. approximated radiation pattern--maximum phase error = 60°

Kbsinθ	F(Kbsinθ)	F'(Kbsinθ)	Ratio	Ratio(dB)
0.000	0.950	0.826	0.869	0.609
0.330	0.933	0.813	0.871	0.598
0.660	0.885	0.777	0.878	0.564
0.989	0.808	0.719	0.890	0.507
1.318	0.708	0.642	0.907	0.425
1.647	0.594	0.551	0.929	0.320
1.976	0.474	0.452	0.953	0.207
2.303	0.360	0.349	0.967	0.146
2.630	0.269	0.247	0.918	0.370
2.957	0.218	0.152	0.698	1.564
3.282	0.214	0.068	0.318	4.981
3.606	0.236	0.002	0.008	20.719
3.929	0.257	0.056	0.217	6.629
4.251	0.265	0.093	0.350	4.562
4.572	0.256	0.113	0.441	3.555
4.891	0.230	0.118	0.511	2.915
5.209	0.191	0.109	0.571	2.431
5.525	0.144	0.090	0.628	2.022
5.840	0.096	0.065	0.671	1.736
6.153	0.063	0.035	0.563	2.496
6.463	0.065	0.005	0.080	10.985
6.772	0.092	0.022	0.246	6.094
7.079	0.117	0.046	0.390	4.093
7.384	0.133	0.062	0.468	3.293
7.686	0.138	0.072	0.522	2.826
7.986	0.132	0.075	0.564	2.489
8.284	0.117	0.070	0.602	2.206
8.579	0.093	0.060	0.640	1.937
8.871	0.066	0.045	0.681	1.666
9.161	0.038	0.027	0.699	1.557

Table 4.5. Actual vs approximated radiation pattern--maximum phase error = 90°

Kbsinθ	F(Kbsinθ)	F'(Kbsinθ)	Ratio	Ratio(dB)
0.000	0.884	0.633	0.716	1.454
0.330	0.869	0.626	0.720	1.424
0.660	0.827	0.608	0.735	1.335
0.989	0.759	0.578	0.761	1.188
1.318	0.674	0.537	0.797	0.984
1.647	0.578	0.488	0.844	0.736
1.976	0.483	0.432	0.895	0.482
2.303	0.400	0.372	0.929	0.319
2.630	0.342	0.309	0.904	0.440
2.957	0.315	0.246	0.782	1.069
3.282	0.313	0.186	0.594	2.264
3.606	0.321	0.130	0.405	3.930
3.929	0.325	0.080	0.246	6.088
4.251	0.318	0.038	0.119	9.253
4.572	0.297	0.004	0.013	18.904
4.891	0.262	0.021	0.082	10.873
5.209	0.217	0.038	0.175	7.572
5.525	0.169	0.047	0.275	5.599
5.840	0.126	0.048	0.382	4.175
6.153	0.100	0.044	0.437	3.597
6.463	0.102	0.035	0.344	4.637
6.772	0.120	0.024	0.196	7.080
7.079	0.140	0.011	0.079	11.030
7.384	0.152	0.001	0.008	20.868
7.686	0.153	0.012	0.078	11.069
7.986	0.145	0.020	0.140	8.530
8.284	0.127	0.026	0.201	6.961
8.579	0.103	0.028	0.268	5.715
8.871	0.075	0.026	0.349	4.572
9.161	0.051	0.022	0.436	3.609

Table 4.6. Actual vs approximated radiation pattern--maximum phase error = 180°

Kbsinθ	F(Kbsinθ)	F'(Kbsinθ)	Ratio	Ratio(dB)
0.000	0.492	0.017	0.035	14.590
0.330	0.490	0.006	0.012	19.136
0.660	0.484	0.026	0.055	12.624
0.989	0.478	0.077	0.162	7.902
1.318	0.475	0.143	0.301	5.217
1.647	0.477	0.217	0.455	3.424
1.976	0.486	0.293	0.604	2.190
2.303	0.499	0.366	0.734	1.343
2.630	0.513	0.430	0.838	0.767
2.957	0.521	0.478	0.916	0.380
3.282	0.522	0.507	0.972	0.123
3.606	0.511	0.515	1.009	0.038
3.929	0.488	0.502	1.027	0.117
4.251	0.456	0.467	1.026	0.111
4.572	0.416	0.415	0.998	0.010
4.891	0.373	0.348	0.931	0.309
5.209	0.335	0.271	0.810	0.917
5.525	0.305	0.190	0.622	2.064
5.840	0.289	0.109	0.379	4.212
6.153	0.284	0.035	0.122	9.131
6.463	0.285	0.030	0.107	9.716
6.772	0.287	0.083	0.288	5.407
7.079	0.285	0.120	0.422	3.748
7.384	0.275	0.142	0.517	2.869
7.686	0.257	0.149	0.579	2.376
7.986	0.233	0.142	0.611	2.142
8.284	0.204	0.124	0.608	2.158
8.579	0.175	0.098	0.559	2.529
8.871	0.151	0.066	0.439	3.572
9.161	0.136	0.033	0.239	6.207

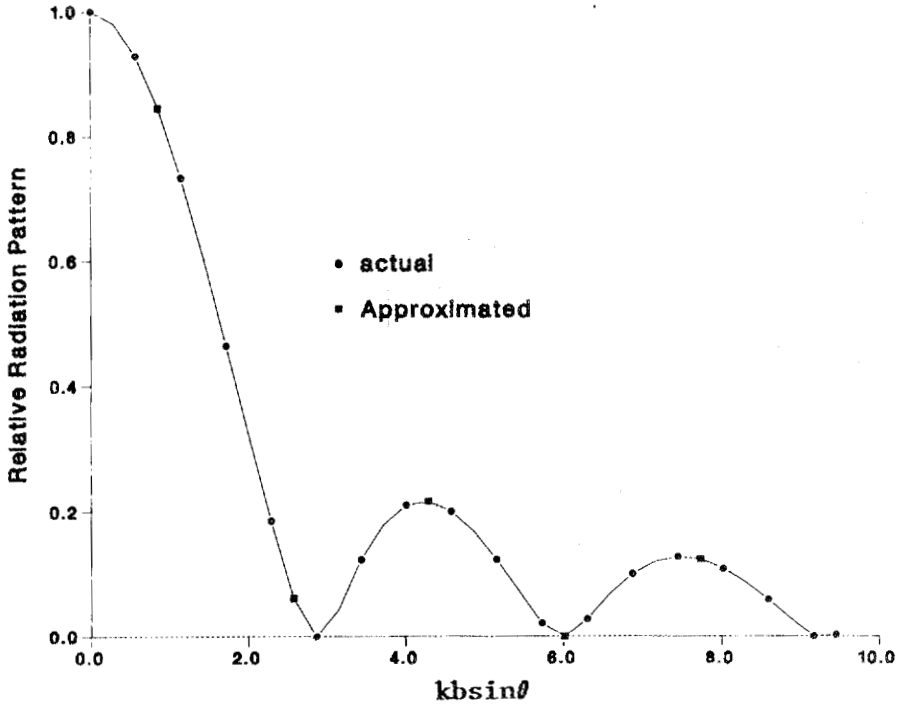

Fig. 4.3. Actual vs approximated radiation pattern--maximum phase error = 0°.

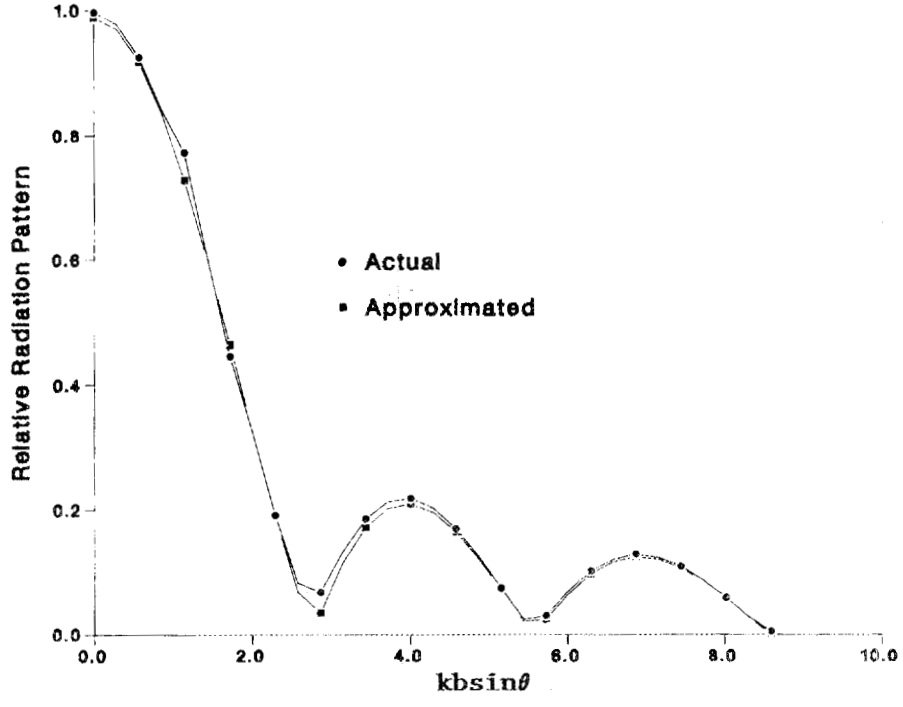

Fig. 4.4. Actual vs approximated radiation pattern--maximum phase error = 15°.

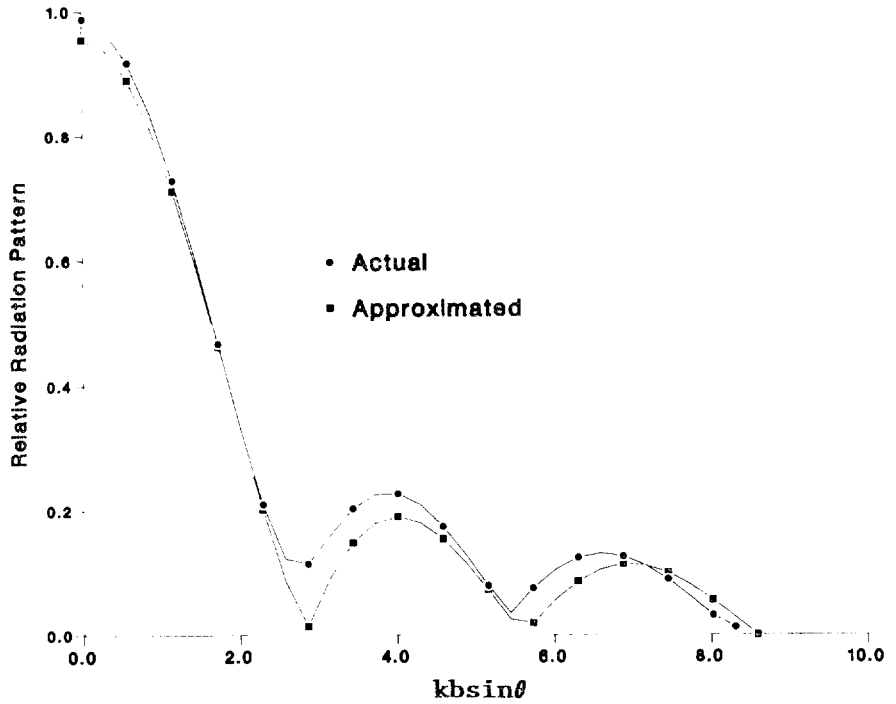

Fig. 4.5. Actual vs approximated radiation pattern--maximum phase error = 30°.

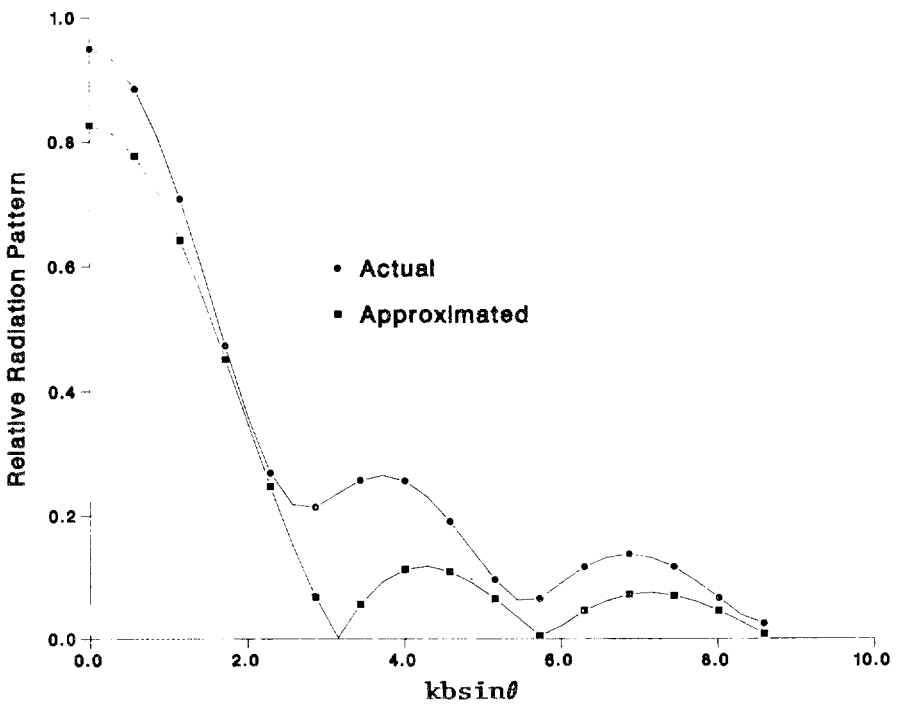

Fig. 4.6. Actual vs approximated radiation pattern--maximum phase error = 60°.

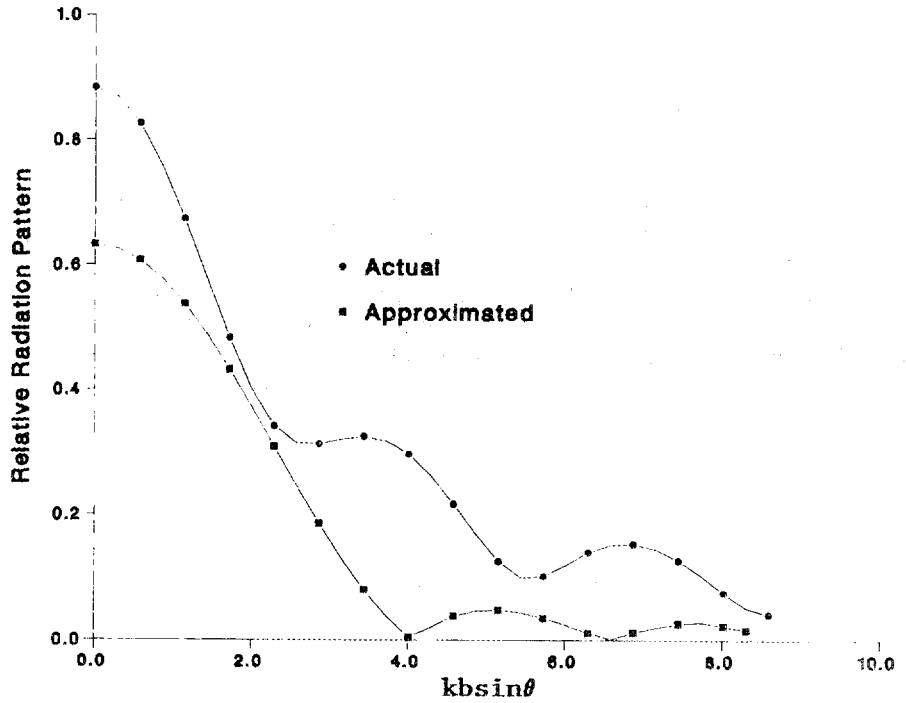

Fig. 4.7. Actual vs approximated radiation pattern--maximum phase error = 90°.

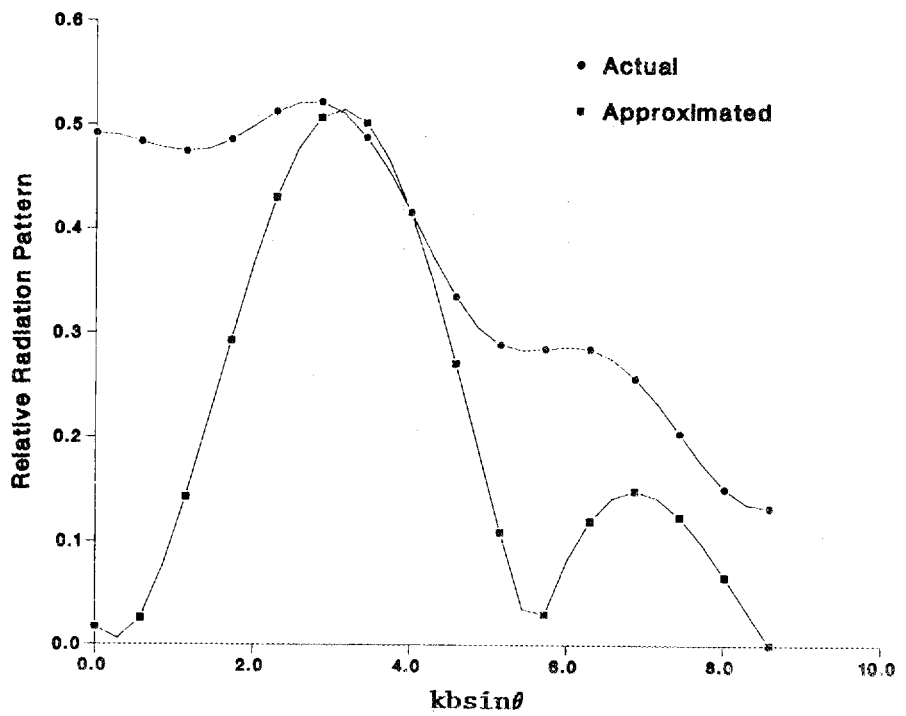

Fig. 4.8. Actual vs approximated radiation pattern--maximum phase error = 180°.

5. SUMMARY

A gain and E field radiation pattern approximation can be used to avoid the complex mathematics and computation methods typically involved in calculating the gain and radiation pattern. A hand-held calculator can be used to solve the trigonometric terms in the approximations, while a computer may be required to calculate the Fresnel integrals in the actual gain equation and perform numerical integration to determine the actual radiation pattern. Also, when an approximation is used, it is important to know how well it is working and what the limitations are. The criterion chosen for a good approximation for these types of power related equations was that the approximated values fall within 3 dB of the calculated values.

For the E-plane horn antenna, the actual gain was

$$G = 8\pi \frac{a/\lambda \ \ell/\lambda}{b/\lambda} \left[C^2(\mu) + S^2(\mu)\right] \quad , \tag{2.12}$$

with

$$\mu = \sqrt{\frac{2}{\lambda\ell}\, b} \quad , \tag{2.11}$$

and the approximated gain was

$$G' = \frac{P_I}{P_E} = 16\pi \ a/\lambda \ b/\lambda \ \frac{\cos^4 \alpha/2}{\cos\alpha} \left[\frac{\sin(\pi \ b/\lambda \ \tan\alpha)}{\pi \ b/\lambda \ \tan\alpha}\right]^2 \quad . \tag{3.23}$$

Tables 3.1 through 3.6 and Figs. 3.2 through 3.7 show that when the flare angle of the E-plane horn antenna is less than 10° for typical antenna dimensions, the 3-dB criterion for the approximation is met. However, the correlation between the actual and approximated gain falls off quickly when the angle flare is 10° or greater. A flare angle less than 10° is reasonable in the design of an antenna.

For the E-plane horn antenna, the actual E field radiation pattern was

$$F(Kb\sin\Theta,\delta) = \frac{1}{2b}\int_{-b}^{b} e^{jK(\sin\Theta Y_s - Y_s^2/2\ell)}\, dY_s \quad , \tag{4.1}$$

and the approximated radiation pattern was

$$F'(Kb\sin\Theta) = \frac{1}{2}\left[\frac{\sin(Kb\sin\Theta')}{Kb\sin\Theta'} + \frac{\sin(Kb\sin\Theta'')}{Kb\sin\Theta''}\right] \quad , \tag{4.6}$$

where

$$\theta' = \frac{\alpha}{2} - \theta \tag{4.4}$$

and

$$\theta'' = \frac{\alpha}{2} + \theta \quad . \tag{4.5}$$

Tables 4.1 through 4.6 and Figs. 4.3 through 4.8 show that when the phase error is 15° or less for the antenna, the approximation criterion for the radiation pattern is met. With no phase error, the approximated radiation pattern is the same as the actual radiation pattern. Except for the regions around the multiples of π, the approximated radiation pattern holds up well until the phase error is over 60°.

6. REFERENCES

1. James D. Tillman, Professor of Electrical Engineering, "Introduction to Antenna Theory," Course Notes, The University of Tennessee, Spring 1986.

2. Edward A. Wolff, *Antenna Analysis*, Wiley, New York, 1966.

3. Warren L. Stutzman, and Gary A. Thiele, *Antenna Theory and Design*, Wiley, New York, 1981.

4. Richard C. Johnson and Henry Jasik, eds., *Antenna Engineering Handbook*, 2d ed, McGraw Hill, New York, 1984.

ORNL/TM-10983
Dist. Category UC-406

INTERNAL DISTRIBUTION

1. H. R. Brashear
2. B. G. Eads
3-7. P. D. Ewing
8. D. N. Fry
9. J. M. Googe
10. W. R. Hamel
11. R. A. Hess
12. D. W. McDonald
13. D. R. Miller
14. O. B. Morgan
15. C. A. Mossman
16. L. C. Oakes
17. R. W. Rochelle
18. R. E. Uhrig
19. J. P. Ball, Advisor
20. P. F. McCrea, Advisor
21-22. Central Research Library
23. Y-12 Document Reference Library
24-25. Laboratory Records
26. Laboratory Records-RC
27. ORNL Patent Section
28. I&C Publications and Information Processing Center

EXTERNAL DISTRIBUTION

29. Assistant Manager for Energy Research and Development, U.S. Department of Energy, Oak Ridge Operations, Oak Ridge, TN 37831.

30-82. Given distribution under Category UC-406, Engineering, Equipment and Instruments.